Journal of Organometallic Chemistry, 338 (1988) 369–382
Elsevier Sequoia S.A., Lausanne – Printed in The Netherlands

Synthesis and molecular structure of diamagnetic heterometallic clusters $(RC_5H_4)_2Cr_2(\mu_3\text{-}S)_2(\mu_4\text{-}S)Co_2(CO)_4$ with a Cr_2Co_2 "butterfly" frame

I.L. Eremenko, A.A. Pasynskii*, B. Orazsakhatov, A.F. Shestakov, G.Sh. Gasanov, A.S. Katugin

*N.S. Kurnakov Institute of General and Inorganic Chemistry, Academy of Sciences of the U.S.S.R.,
31 Leninsky Prospect, Moscow V-71 (U.S.S.R.)*

Yu.T. Struchkov and V.E. Shklover

*A.N. Nesmeyanov Institute of Organoelement Compounds, Academy of Sciences of the U.S.S.R.,
28 Vavilov Str., Moscow V-312 (U.S.S.R.)*

(Received July 1st, 1987)

Abstract

The interaction of $(RC_5H_4)_2Cr_2(SCMe_3)_2(\mu\text{-}S)$ (I, R = H; Ia, R = CH_3) with $Co_2(CO)_8$ in a molar ratio of 1/1 gave the 62-electron, heteronuclear clusters $(RC_5H_4)_2Cr_2(\mu_3\text{-}S)_2(\mu_4\text{-}S)Co_2(CO)_4$ (II and IIa respectively), which were characterized by X-ray crystallography. Crystals of II are monoclinic, space group $C2/c$, a 15.246(1), b 11.846(9), c 9.9434(6) Å, β 100.965(6)°, V 1763 Å^3, $Z = 4$, $R = 0.046$, $R_w = 0.057$. Crystals of IIa are triclinic, space group $P\bar{1}$, a 9.9771(9), b 10.1120(10), c 11.0770(10) Å, α 116.982(8), β 99.560(8), γ 82.054(8)°, V 979.5 Å^3, $Z = 2$, $R = 0.064$, $R_w = 0.060$. The two clusters have a Cr_2Co_2 "metal butterfly" framework. In II, the Cr–Cr separation is 2.544(1) Å and those of Cr–Co are 2.622(1) and 2.617(1) Å, the dihedral angle between the Cr_2Co wings of the butterfly is 124.2°. The μ_3-sulphide bridge is situated below each wing whereas the μ_4-sulphide bridge is located between the wings. The average distances are: Cr–(μ_3-S), 2.258(2), Cr–(μ_4-S), 2.326(2), Co–(μ_3-S), 2.178(2), Co–(μ_4-S) 2.205(2) Å. The geometry of IIa differs from II in that it has the staggered ring conformation instead of the eclipsed, it has non-equivalent Co–Cr bonds (av. 2.634(2) and 2.614(2) Å) and has slightly shortened Co–(μ_4-S) bonds (av. to 2.193(3) Å). The structures of II and IIa were compared with the geometries of previously studied clusters, viz. the 66-electron "metal chain" $Cp_2Cr_2(\mu_3\text{-}S)_2(\mu_4\text{-}S)Ni_2Cp_2$ and 62-electron "metal butterfly" $Cp_2Mo_2(\mu_3\text{-}S)_2(\mu_4\text{-}S)Co_2(CO)_4$.

0022-328X/88/$03.50

Introduction

We have previously investigated the tetranuclear heterometallic cluster, $Cp_4Cr_2Ni_2(\mu_3\text{-}S)_2(\mu_4\text{-}S)$ ($Cp = \pi\text{-}C_5H_5$), which contains the framework of a non-symmetrical "metal butterfly" with a short Cr–Cr bond of 2.62(1) Å and paired non-equivalent Cr–Ni bonds of (2.64(1) and 2.86(1) Å) [1]. This cluster has 66 electrons instead of 62, the usually number found "butterfly" structures. Four "additional" electrons probably occupy the antibonding orbitals of Cr–Ni bonds, so it is more correct to regard this structure as a "metal chain" Ni–Cr–Cr–Ni, in which the Ni–Cr distances (2.86(1) Å) are probably antibonding. The analogous non-equivalence of the M–Cr bonds observed previously in the triangular cluster $(Cp_2Cr_2SCMe_3)(\mu_3\text{-}S)_2Fe(CO)_3$ with the ordinary (two-electron) and half (one electron per antibonding orbital) Cr–Fe bonds which are 2.726(2) and 3.110(2) Å, respectively [2]. Non-equivalence of the M–Cr distances decreased sharply during the transition to the manganese-containing analogue $(Cp_2Cr_2SCMe_3)(\mu_3\text{-}S)_2Mn(CO)_3$, i.e. during formal removal of an electron from the antibonding orbitals of the M–Cr bonds. In this case the Mn–Cr bonds are approximately equal, 2.716(2) and 2.828(2) Å, the small difference is due to the non-symmetrical disposition of the $Mn(CO)_3$ group relative to the $Cr_2(\mu_3\text{-}S)_2$ fragment [3]. When this non-symmetry is removed by replacement of $Mn(CO)_3$ by an isoelectronic fragment $Co(CO)_2$ in complex $(Cp_2Cr_2SCMe_3)(\mu_3\text{-}S)_2Co(CO)_2$, the Cr–Co distance turn out equal (2.586(1) Å) [4].

The effect of removing the electrons from the antibonding orbitals of "metal-chain" by formal replacement of two 15-electronic CpNi fragments by 13-electronic $Co(CO)_2$ fragments in the cluster $(RC_5H_4)_2Cr_2(\mu_3\text{-}S)_2(\mu_4\text{-}S)Co(CO)_4$ (II, where R = H) was of great interest. To increase the reliability of the information obtained, and to estimate the influence of methyl substituents in rings, the analogous cluster IIa (with $R = CH_3$) was also studied.

Results

Cluster II was obtained by applying moderate heat to equimolar quantities of $(CpCrSCMe_3)_2S$ (I) and $Co_2(CO)_8$ in benzene:

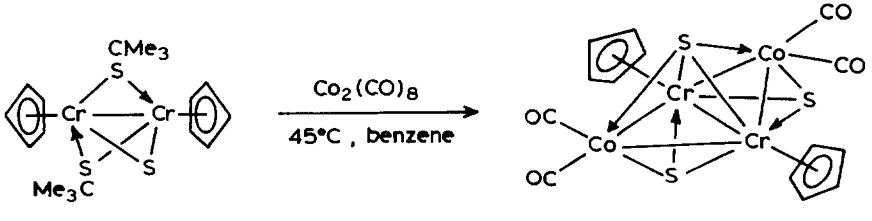

(I) (II)

Black-brown crystals of II crystallized from the reaction solution. The IR spectrum of II shows the bands due to vibrations of the terminal CO groups (at 1940 and 1980 cm^{-1}), and vibrations typical of C_5H_5 rings. For objective determination of the structure of complex II an X-ray diffraction study was carried out (Tables 1–3).

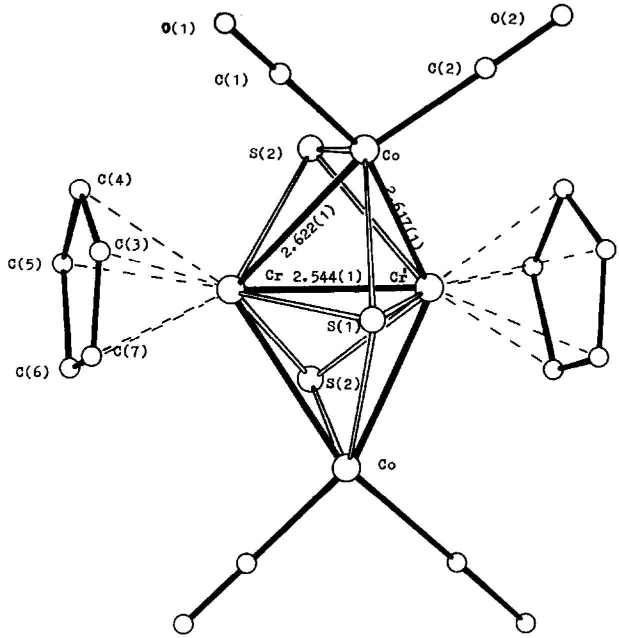

Fig. 1. The molecular structure of $(C_5H_5)_2Cr_2(\mu_3\text{-}S)_2(\mu_4\text{-}S)Co_2(CO)_4$ (II).

The molecule of cluster II (Fig. 1, 2) is situated on the crystallographic two-fold axis, with the tetradentate S(1) atom having the coordinates 0, y, 1/4). The metal atoms form a "butterfly" framework in which the Cr–Cr axis of 2.544(1) Å, the $Co\text{-}Cr_2$ "wings" are 2.622(1) and 2.617(1) Å, and the dihedral angle of the frame is 124.2°. The Co · · · Co separation 4.047(1) Å is non-bonded. The terdentate bridge sulphur atom is placed below each $CoCr_2$ wing with Co–S distances of 2.178(2) Å, Cr–S distances of 2.265(2) and 2.253(2) Å. The tetradentate sulphide bridge is located between the wings at an average Co–S distance of 2.205(1) Å and Cr–S distance of 2.326(2) Å. Each Cr atom is also coordinated by a cyclopentadienyl ligand at an average Cr–C distance of 2.233(8) Å and with C–C distances of 1.40(1) Å, and a (centre of C_5H_5 ring)–Cr–Cr angle approaching 180°. Each Co atom is bonded in turn to two terminal carbonyl groups (average distance: Co–C, 1.789(7); C–O 1.131(9) Å), the CoS_2 plane is almost normal to the $CoCr_2$ plane (dihedral angle 91.3°). When Co–Cr bonds are neglected, each Co atom has a distorted tetrahedral surrounding.

The methylcyclopentadienyl cluster IIa ($R = CH_3$) was obtained by the analogous reaction of equimolar quantities of $(CH_3C_5H_4CrSCMe_3)_2S$ (Ia) with $Co_2(CO)_8$ in benzene/heptane mixture at room temperature. From static magnetic susceptibility measurements IIa was found to be diamagnetic. The IR spectrum of IIa contains only two intense bands due to terminal carbonyl group vibrations (at 1945 and 1975 cm^{-1}) indicating $Co(CO)_2$ fragment equivalence. From X-ray data (Fig. 3, Tables 4–6) cluster IIa was seen to have almost the same metal butterfly framework as II, although the methylcyclopentadienyl ligands in IIa are arranged in a staggered conformation in contrast to the eclipsed conformation of unsubstituted C_5H_5

(*Continued on p. 374*)

Table 1

Atomic coordinates (for Co, Cr and S multiplied by 10^5; for the other atoms by 10^4) and anisotropic temperature factors in the form $T = \exp -1/4(B_{11}h^2a^{*2} + \ldots + 2B_{23}klb^*c^*)$ for molecule II

Atom	x	y	z	B_{11}	B_{22}	B_{33}	B_{12}	B_{13}	B_{23}
Co	−12183(6)	33362(8)	12626(9)	2.73(3)	2.24(3)	2.42(4)	0.18(3)	0.36(3)	0(3)
Cr	3662(7)	24314(8)	14523(10)	2.64(4)	1.68(3)	1.64(3)	0.09(3)	0.90(3)	0.07(3)
S(1)	0	40749(17)	1/4	2.94(9)	1.61(8)	2.56(9)	0	0.57(7)	0
S(2)	−9327(11)	15432(13)	15693(1)	3.23(6)	2.01(6)	2.46(6)	−0.41(5)	0.86(5)	−0.41(5)
O(1)	−1681(4)	3876(5)	−1654(6)	5.7(3)	6.4(3)	3.5(3)	−0.5(3)	−0.2(2)	1.5(3)
O(2)	−2925(3)	3989(5)	1947(7)	3.5(2)	6.6(3)	6.5(4)	1.1(2)	0.7(2)	−1.3(3)
C(1)	−1500(5)	3680(6)	−524(8)	4.1(3)	2.7(3)	3.5(3)	0.0(2)	0.2(3)	0.3(3)
C(2)	−2259(5)	3738(6)	1693(8)	3.2(3)	3.2(3)	3.9(4)	0.3(3)	0.1(3)	−0.4(3)
C(3)	903(6)	1300(6)	35(8)	6.9(5)	3.4(3)	3.3(3)	0.7(3)	3.2(3)	−0.6(3)
C(4)	1602(5)	1998(7)	658(8)	3.8(3)	5.3(4)	3.4(3)	1.2(3)	2.2(3)	0.4(3)
C(5)	1361(5)	3111(7)	243(8)	4.7(4)	4.5(4)	3.3(3)	−0.8(3)	2.5(3)	0.0(3)
C(6)	541(5)	3084(7)	−594(8)	6.0(4)	4.8(4)	3.0(3)	1.3(3)	2.9(3)	1.7(3)
C(7)	226(5)	1961(7)	−742(7)	4.9(4)	6.5(5)	1.9(3)	−1.1(4)	1.7(3)	−0.9(3)

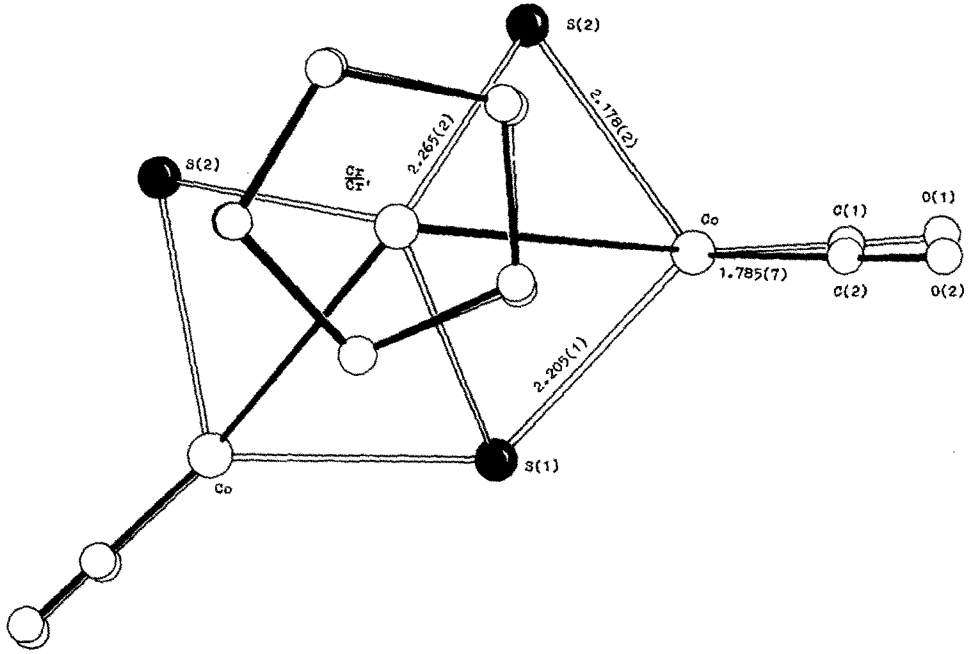

Fig. 2. The projection of the molecule II along the Cr–Cr axis.

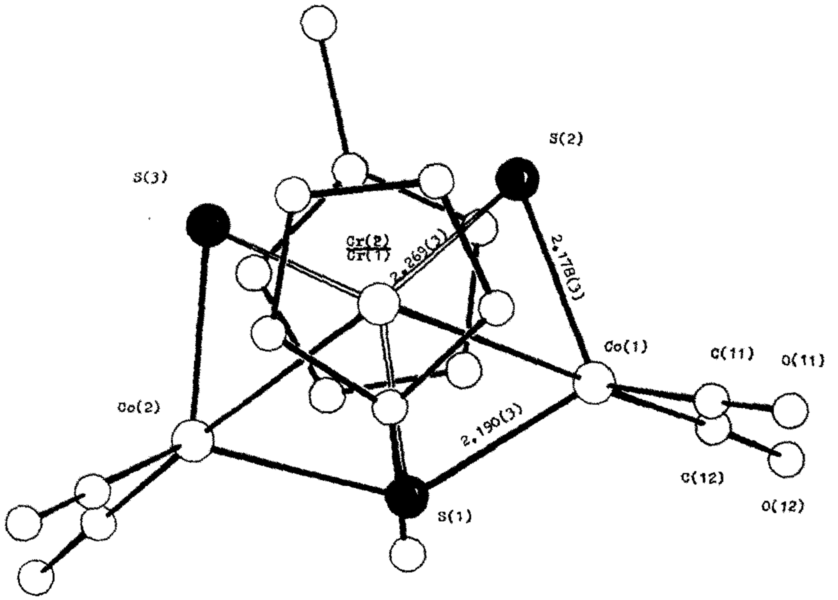

Fig. 3. The projection of the molecule $(MeC_5H_4)_2Cr_2(\mu_3\text{-}S)_2(\mu_4\text{-}S)Co_2(CO)_4$ (IIa) along the Cr–Cr axis.

ligands in II. Some non-equivalence of the Cr–Co bonds (av. 2.634(2) and 2.614(2) Å) may be accounted for by short non-covalent contacts $CH_3 \cdots S$ (2.935 Å). The bond length Cr–Cr (2.544(1) Å) remains the same as in II. Some shortening of the Co–(μ_4-S) bonds (av. to 2.193(3) Å) can also be seen.

Discussion

The formation of clusters II and IIa with the metal butterfly Cr_2Co_2 frameworks, resulting from the reaction of I (or Ia) and $Co_2(CO)_8$, according to reaction mixture IR data, proceeds via the intermediate trinuclear cluster $(RC_5H_4)_2Cr_2(\mu\text{-}SCMe_3)(\mu_3\text{-}S)_2Co(CO)_2$ (III, R = H [4]; IIIa, R = CH_3 [5]) studied by us previously:

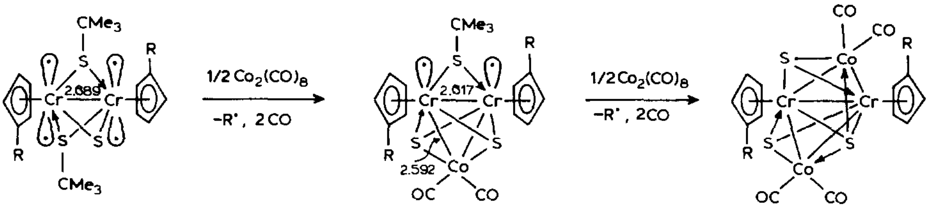

(I, Ia) (III, IIIa) (II, IIa)

In both cases the I → III and III → II transitions are probably start by donor–acceptor bonding of coordinatively unsaturated $Co(CO)_3$ fragment to the lone electron pair of the μ_2- or the μ_3-sulphide bridge, respectively. In each case the CMe_3 group is replaced, and second Co–S bond is formed along with new Co–Cr bonds.

This way of $Co(CO)_3$ fragment attachment is analogous to that for the bonding of other $M(CO)_3$ fragments ($M = Mn^I$ [3] or Fe^1 [2] with the electronic configuration of d^6 or d^7, respectively). However in this case the transition to $M = Co^I$ with the d^8 electronic configuration leads to the appearance of two or four electrons on the antibonding orbitals of the Co–Cr bonds in the possible intermediates $(Cp_2Cr_2SCMe_3)(S)_2Co(CO)_3$ or $Cp_2Cr_2(S)_3Co_2(CO)_6$ respectively. The last complex is the electronic analogue of $Cp_2Cr_2(S)_3Ni_2Cp_2$ [I], which has the "metal chain" structure with two short and two long Cr–Ni bonds (see Introduction). In the case of intermediate $Cp_2Cr_2(S)_3Co_2(CO)_6$ four additional electrons are lost when the two carbonyl groups are removed and so all four of the Co–Cr bonds in II and IIa are short and nearly equal. $Cp_2Mo_2(\mu_3\text{-}S)_2(\mu_4\text{-}S)Co_2(CO)_4$, which results from the reaction of $Cp_2Mo_2(S)_2(SH)_2$ with cobalt carbonyl cluster, was found to have the same structure, with the "butterfly" Mo_2Co_2 framework [6]. In this compound the lengthening of the Mo–Mo bonds to 2.646 Å, Mo–Co bonds to 2.64 Å, Mo–(μ_3-S) bonds to 2.362 Å, and Mo–(μ_4-S) bonds to 2.390 Å was observed as compared to the corresponding chromium–element distances in II, these increases are possibly due to the greater covalent radius of molybdenum atom.

In order to determine which type of orbital of the chromium atom participate in the metal–metal interactions, and to gain an insight into the peculiarities of Cr–S and Cr–C_5H_4R bonding, the calculation of electronic structure of $Cp_2Cr_2(\mu_3$-

Table 2

Bond lengths d (Å) in the molecule $(C_5H_5)_2Cr_2(\mu_3\text{-}S)_2(\mu_4\text{-}S)Co_2(CO)_4$ (II)

Bond	d (Å)	Bond	d (Å)
Co–Cr	2.622(1)	Cr–C(4)	2.237(8)
Co–Cr′	2.617(1)	Cr–C(5)	2.255(8)
Co–S(1)	2.205(1)	Cr–C(6)	2.240(8)
Co–S(2)	2.178(2)	Cr–C(7)	2.222(7)
Co–C(1)	1.793(7)	O(1)–C(1)	1.130(9)
Co–C(2)	1.785(7)	O(2)–C(2)	1.132(9)
Cr–Cr′	2.326(2)	C(3)–C(7)	1.40(1)
Cr–S(2)	2.265(2)	C(4)–C(5)	1.41(1)
Cr–S(2)	2.253(2)	C(5)–C(6)	1.36(1)
Cr–C(3)	2.212(8)	C(6)–C(7)	1.41(1)

Table 3

Bond angles ω (degrees) in the molecule II

Angle	ω	Angle	ω
CrCoCr	58.11(4)	S(2)CrS(2)	86.10(7)
CrCoS(1)	56.91(4)	CoS(1)Co	133.23(7)
CrCoS(1)	56.82(4)	CoS(1)Cr	70.51(5)
CrCoS(2)	55.47(5)	CoS(1)Cr	70.68(5)
CrCoS(2)	55.05(5)	CrS(1)Cr	66.32(5)
S(1)CoS(2)	100.61(6)	CoS(2)Cr	72.14(6)
C(1)CoC(2)	96.9(3)	CoS(2)Cr	72.55(6)
CoCrCo	101.15(4)	CrS(2)Cr	68.54(6)
CoCrCr	61.06(4)	CoC(1)O(1)	178.7(7)
CoCrCr	60.84(4)	CoC(2)O(2)	179.0(7)
CoCrS(1)	52.58(4)	C(4)C(3)C(7)	109.4(7)
CoCrS(1)	52.50(4)	C(3)C(4)C(5)	106.8(7)
CrCrS(1)	56.84(4)	C(4)C(5)C(6)	108.4(7)
CoCrS(2)	52.39(5)	C(5)C(6)C(7)	109.8(7)
CoCrS(2)	116.06(6)	C(6)C(7)C(3)	105.6(7)
S(1)CrS(2)	94.54(6)		

$S)_2(\mu_2\text{-}SCMe_3)^-$ was calculated by use of the Extended Hückel Method * [7,8].

Interestingly, the linear structure of CpCr–CrCp group is retained and the overall geometry of $Cp_2Cr_2S_3$ fragments changes little in the series I, III and II. Thus the calculated results may be used to estimate the bonding of these fragments in all of the complexes I–III. From these calculations, a scheme of the molecular orbitals was built up from the orbitals of mononuclear CpCr fragments and is depicted in Fig. 4.

Strong interaction of the chromium atoms with the cyclopentadienyl ligands splits the d-orbital set into three groups: weakly-bonding (relative to Cp–Cr bond) $d_{x^2-y^2,xy}$ orbitals, weakly-antibonding d_{z^2} and antibonding $d_{xz,yz}$ orbitals. Subsequent interaction with the lower-lying p-orbitals of the bridge S atoms results in the

---

* The geometrical parameters were taken on the basis of X-ray data [4]. The following values of quantum chemistry parameters were used; the ionization potentials and exponents: 13.6, 1.30 (H 1s), 21.4, 1.625 (C 2s), 11.4, 1.625 (C 2p), 20.0, 1.817 (S 3s), 13.3, 1.817 (S 3p), 11.22, 4.95 (weight 0.48761) and 1.60 (weight 0.72051) (Cr 3d), 8.66, 1.70 (Cr 4s), 5.24, 1.70 (Cr 4p).

Table 4

Atomic coordinates (for Co, Cr, S and O multiplied by 10^4; for C by 10^3) and anisotropic temperature factors in the form $T = \exp[-1/4(B_{11}h^2a^{*2} + \ldots + 2B_{23}klb^*c^*)]$ for the molecule IIa

Atom	x	y	z	B_{11}	B_{22}	B_{33}	B_{12}	B_{13}	B_{23}
Co(1)	1967(2)	371(2)	4520(2)	3.30(7)	1.66(6)	2.46(6)	−0.38(5)	−0.22(5)	0.81(5)
Co(2)	4519(2)	385(2)	2053(2)	3.07(7)	1.90(6)	2.99(7)	−0.38(5)	−0.05(5)	0.96(5)
Cr(1)	1959(2)	1138(2)	2543(2)	2.84(7)	1.06(6)	2.36(7)	−0.06(5)	−0.36(6)	0.75(5)
Cr(2)	3018(2)	−1407(2)	2268(2)	2.89(7)	0.94(6)	2.33(7)	−0.14(5)	−0.43(6)	0.59(5)
S(1)	3827(3)	792(3)	3981(3)	3.1(1)	1.7(1)	2.3(1)	−0.6(1)	−0.7(1)	0.7(1)
S(2)	792(3)	−641(3)	2520(3)	2.9(1)	1.8(1)	3.1(1)	−0.6(1)	−0.5(1)	0.9(1)
S(3)	2751(3)	−621(3)	618(3)	3.5(1)	1.8(1)	2.5(1)	−0.1(1)	−0.4(1)	0.8(1)
O(11)	2069(9)	−1562(9)	5850(9)	5.7(5)	3.7(4)	4.9(4)	−0.3(3)	0.1(4)	2.8(4)
O(12)	691(9)	2989(9)	6635(9)	6.7(5)	2.7(3)	4.1(4)	0.0(3)	1.4(4)	0.4(3)
O(21)	6966(9)	−1552(9)	1160(9)	4.3(4)	4.8(4)	6.7(5)	1.0(3)	1.4(4)	2.8(4)
O(22)	5478(9)	3021(8)	2084(9)	7.9(6)	3.0(4)	6.9(5)	−1.8(4)	1.5(5)	1.9(4)
C(11)	208(1)	−81(1)	534(1)	3.6(5)	2.9(5)	2.8(5)	−0.6(4)	−0.6(4)	0.9(4)
C(12)	118(1)	198(1)	581(1)	3.5(5)	3.3(5)	2.9(5)	−1.2(4)	−0.2(4)	1.4(4)
C(21)	602(1)	−79(1)	153(1)	3.7(5)	3.3(5)	3.6(5)	−0.9(4)	−0.1(4)	1.6(4)
C(22)	508(1)	201(1)	204(1)	5.0(6)	3.7(5)	3.2(5)	−1.1(5)	−0.1(5)	1.6(5)
C(13)	−3(1)	238(1)	227(1)	4.2(6)	2.4(5)	5.4(7)	0.7(4)	−0.8(5)	2.3(5)
C(14)	82(1)	233(1)	137(1)	5.4(7)	2.5(5)	4.6(6)	1.1(4)	−0.8(5)	1.9(5)
C(15)	200(1)	313(1)	217(1)	5.1(6)	1.8(4)	5.7(6)	1.3(4)	0.8(5)	2.6(5)
C(16)	183(1)	366(1)	356(1)	4.3(6)	0.8(4)	4.9(6)	0.8(4)	−0.2(4)	1.1(4)
C(17)	59(1)	319(1)	363(1)	4.6(6)	1.7(4)	4.6(6)	1.2(4)	0.6(5)	1.7(4)
C(18)	280(1)	457(1)	479(1)	7.0(8)	1.7(5)	5.8(8)	−1.4(5)	−2.0(6)	0.4(5)
C(23)	391(1)	−304(1)	312(1)	4.5(6)	1.2(4)	4.7(6)	0.7(4)	−0.3(5)	1.5(4)
C(24)	484(1)	−299(1)	232(1)	4.2(6)	1.2(4)	4.7(6)	0.6(4)	0.0(5)	1.4(4)
C(25)	422(1)	−347(1)	96(1)	5.5(6)	0.9(4)	4.2(6)	0.9(4)	0.4(5)	0.9(4)
C(26)	290(1)	−386(1)	90(1)	6.3(7)	0.4(4)	4.2(6)	0.5(4)	−1.3(5)	0.5(4)
C(27)	266(1)	−358(1)	225(1)	4.8(6)	1.1(4)	5.5(7)	0.1(4)	−0.4(5)	1.6(4)
C(28)	185(1)	−447(1)	−38(1)	9.7(10)	1.8(5)	6.6(8)	−1.1(6)	−5.2(8)	0.2(5)

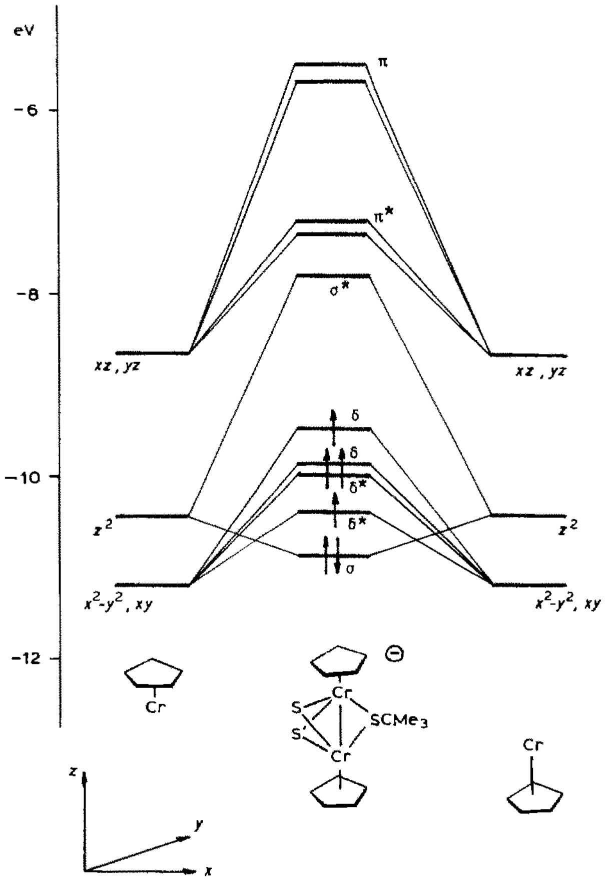

Fig. 4. The scheme of $Cp_2Cr_2S_2SR^-$ fragment molecular orbitals forming (the Cr–S bond orbitals are omitted).

destabilization of the d-levels. The unusual sequence of level, viz. $\delta(d\text{–}d) > \delta^*(d\text{–}d)$ and $\pi(d\text{–}d) > \pi^*(d\text{–}d)$ and is the consequence of greater Cr–S interactions compared with Cr–Cr interactions. The main localization of Cr–Cr bond orbitals is directed by the Cr–S interaction, so that the $\delta(d\text{–}d)$ orbitals are formed by the participation of both the p_x and the p_y orbitals of the S atom in the local coordinate system, whereas the $\delta^*(d\text{–}d)$ orbitals are formed only by participation of the p_z-orbitals of S atom (Fig. 5). The situation for $\pi(d\text{–}d)$ and $\pi^*(d\text{–}d)$ orbitals is analogous, but additional destabilization of these orbitals is present owing to interaction with S atom s-orbitals.

As to the "normal" sequence of orbitals $\sigma(d\text{–}d) < \sigma^*(d\text{–}d)$, this does not follow from an essentially greater Cr–Cr interaction strength, because overlapping integrals of different types are comparable: $\langle d_\sigma/d_\sigma\rangle = 0.0905$, $\langle d_\pi/d_\pi\rangle = -0.0945$, $\langle d_\delta/d_\delta\rangle = 0.0232$. Rather it is accounted for by the smaller destabilization of the σ-orbitals, which interact only with the p_y-orbitals of sulphur atoms, compared with the destabilization of σ^*-orbitals, which interact with the p_z-orbitals of the S atoms. This follows from a comparison of the overlapping integrals $\langle \mathrm{Cr}(d_\sigma)/\mathrm{S}(p_y)\rangle = -0.052$, $\langle \mathrm{Cr}(d_{\sigma^*})/\mathrm{S}(p_z)\rangle = 0.082$. It is noteworthy that overlapping with the s-

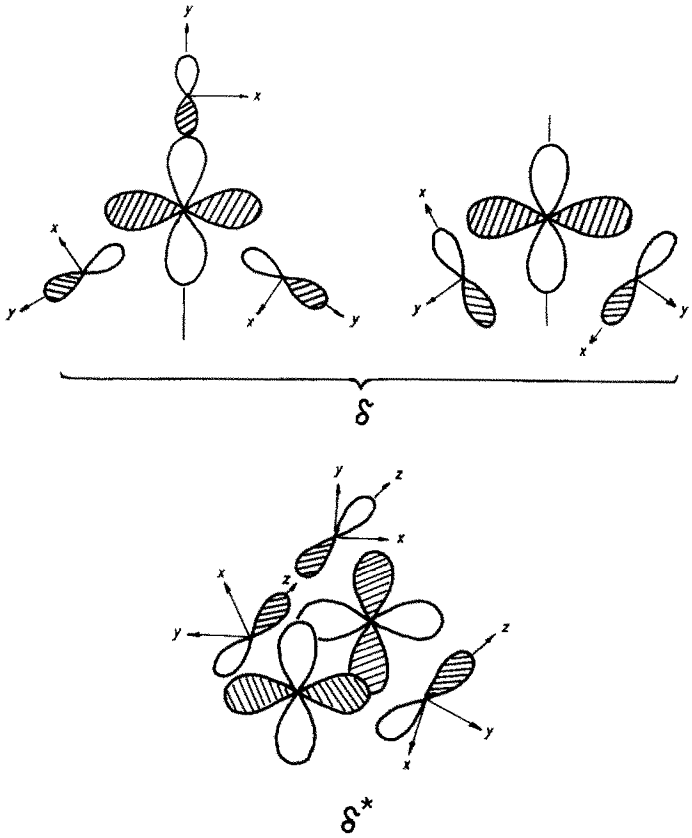

Fig. 5. The interaction of Cr atom *d*-orbitals with the S atom *p*-orbitals, destabilizing δ and δ^* orbitals of the Cr–Cr bond.

orbitals of the S atom is non-effective, because they are situated nearly the nodes of the d_σ orbitals.

As shown in Fig. 4, the $\delta(d\text{–}d)$ and $\delta^*(d\text{–}d)$ levels are split weakly, so that uncoupling of the electrons owing to inter-electronic interaction effects can be expected. Accounting of these interactions in the local Hamiltonian-spin model resulted in:

$$J = -J_{\mathrm{Cr}} \sum_{i=1}^{2} \langle S_i^2 \rangle$$

Here $\langle S_i^2 \rangle$ is the mean value of local spin operator of the i^{th} Cr atom, calculated from the effective number of unpaired electrons n_i (from Mulliken's analysis) of the i^{th} center $\langle S_i^2 \rangle = n_i/2(n_i/2 + I)$. The value of J_{Cr} can also be expressed through the B and C Racah parameters such that: $J_{\mathrm{Cr}} = 7/I2(5B + 2C)$. The numerical value of J_{Cr} for Cr^{3+} in light of published data [9] equals 0.93 eV.

The total energy change $\Delta E + J$, consisting from energy expenses for the electron excitation on high energy orbitals ΔE and energy gain due to one-center interaction (J) are equal 0.808, 1.123 and 0.036 eV for uncoupling of 2, 4 and 6 electrons

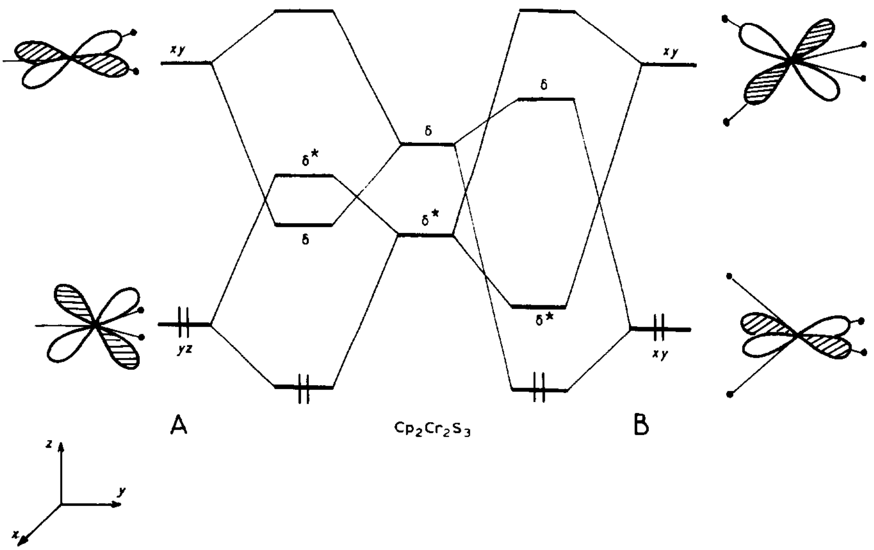

Fig. 6. The interaction of the frontier orbitals of $Co(CO)_3$ and NiCp (A) and $Co(CO)_2$ fragments (B) with δ and δ* orbitals of the $Cp_2Cr_2S_3$ fragment.

respectively. Thus, the $Cp_2Cr_2SCMe_3(S)_2^-$ fragment in ground state has four unpaired electrons and the $(\sigma)^2(\delta^*)^2(\delta)^2$ electron configuration.

The use of all four half occupied orbitals of di-chromium fragment for the forming of Co–Cr bonds with two $Co(CO)_2$ fragments, probably explains diamagnetic properties of clusters II and IIa, in contrast to I and Ia or III and IIIa, possessing antiferromagnetic properties because of half occupied chromium orbitals.

It was of interest to us to compare the bonding character in the diamagnetic cluster $Cp_2Cr_2S_3Co_2(CO)_4$ (II), with that of antiferromagnetic cluster $Cp_2Cr_2S_3Ni_2Cp_2$ described by us (see Introduction), and with its hypothetical isoelectronic analogue $Cp_2Cr_2S_3Co_2(CO)_6$.

There is significant difference in the interaction of the δ and δ* orbitals of Cp_2Cr_2 fragment with the *d*-orbitals of the $(OC)_2CoS_2$ fragments on one hand and isoelectronic $(OC)_3CoS_2$ and $CpNiS_2$ fragments on the other. The reason is that in first case the lowest vacant *d*-orbital (d_{yz}) is oriented in the MCr_2 plane and in the second case the corresponding orbital is normal to the (d_{xy}) plane (Fig. 6).

The highest occupied orbitals of Co- and Ni-containing fragments, are oriented in the opposite manner, *d*-orbitals of the $(OC)_2CoS_2$ fragment are normal to the Cr_2Co (d_{xy}) plane and *d*-orbital of the $(OC)_3CoS_3$ or $CpNiS_2$ fragment (d_{yz}) is in the Cr_2M plane (M = Co, Ni) (Fig. 6).

On conditions of symmetry, the d_{xy}-orbitals of ML_n interact with δ-orbitals of Cr_2, and the d_{yz}-orbitals interact with δ*-orbitals. In the case of the $Co(CO)_2$ fragment this leads to the destabilization of δ- and stabilization of δ*-orbitals (Fig. 6). Because of this δ–δ* splitting increases which accounts for strengthening of the antiferromagnetic interactions up to the transition to the diamagnetic state. In contrast, $Co(CO)_3$ or CpNi fragment δ-orbitals were stabilized and δ*-orbitals were destabilised, which confirms that there is only a small gap between these states, so that antiferromagnetic properties are retained.

Table 5

Bond lengths, d (Å) in the molecule $(\mathrm{MeC_5H_4})_2\mathrm{Cr_2}(\mu_3\text{-S})_2(\mu_4\text{-S})\mathrm{Co_2(CO)_4}$ (IIa)

Bond	d (Å)	Bond	d (Å)
Co(1)–Cr(1)	2.632(2)	Cr(1)–C(15)	2.24(1)
Co(1)–Cr(2)	2.614(2)	Cr(1)–C(16)	2.27(1)
Co(1)–S(1)	2.190(3)	Cr(1)–C(17)	2.26(1)
Co(1)–S(2)	2.178(3)	Cr(2)–S(1)	2.314(3)
Co(1)–C(11)	1.78(1)	Cr(2)–S(2)	2.269(3)
Co(1)–C(12)	1.79(1)	Cr(2)–S(3)	2.267(3)
Co(2)–Cr(1)	2.636(2)	Cr(2)–C(23)	2.26(1)
Co(2)–Cr(2)	2.615(2)	Cr(2)–C(24)	2.26(1)
Co(2)–S(1)	2.197(3)	Cr(2)–C(25)	2.25(1)
Co(2)–S(3)	2.184(3)	Cr(2)–C(26)	2.26(1)
Co(2)–C(21)	1.78(1)	Cr(2)–C(27)	2.26(1)
Co(2)–C(22)	1.81(1)	C(11)–O(11)	1.14(2)
Cr(1)–Cr(2)	2.544(2)	C(12)–O(12)	1.13(2)
Cr(1)–S(1)	2.340(3)	C(21)–O(21)	1.14(2)
Cr(1)–S(2)	2.262(3)	C(22)–O(22)	1.13(2)
Cr(1)–S(3)	2.251(3)	C–C($\mathrm{C_5H_4}$) (average)	1.42(2)
Cr(1)–C(13)	2.25(1)		
Cr(1)–C(14)	2.23(1)	C–Me (average)	1.53(2)

The contracting changes in the M–(μ_4-S) and Cr–(μ_4-S) bond lengths are also a unique feature of complexes containing $\mathrm{Co(CO)_2}$ or CpNi fragments: for M = Co these bond lengths equal 2.20 and 2.31 Å and for M = Ni 2.30 and 2.24 Å, respectively. This dependence may be explained in terms of the difference in donor–acceptor properties of $\mathrm{Co(CO)_2}$ fragments, having electron acceptor CO groups, and CpNi fragments, having mainly electron donor $\mathrm{C_5H_5}^-$ ligand. In the first case withdrawal of the electron density from μ_4-S atom to the Co atoms must apparently strengthen the Co–(μ_4-S) bonds and weaken the Cr–(μ_4-S) bonds, whereas in the second case the Ni–(μ_4-S) bonds must have been weakened and the Cr–(μ_4-S) bonds must have been strengthened.

In conclusion it should be noted, that the use in bonding with chromium atoms of all four (s, p_x, p_y and p_z) orbitals of sulphide bridges means the participation of formally unshared electron pairs of sulphur atoms in "double-bonding" $\overleftarrow{\mathrm{Cr}-\ddot{\mathrm{S}}}$. This agrees with the decrease in Cr–S distances to 2.25–2.30 Å, which is essentially less than the sum of the covalent radii of Cr (1.46 Å [10]) and S (1.04 Å) atoms. Furthermore, these values of Cr–S bond lengths are intermediate between observed for the strong $\overleftarrow{\mathrm{Cr}-\ddot{\mathrm{S}}}$ double-bonding in electron deficient complex $\mathrm{Cp(CO)_2}\overleftarrow{\mathrm{Cr}-\ddot{\mathrm{S}}}-\mathrm{Cr}-\mathrm{(CO)_2Cp}$ (Cr–S 2.07 Å) [11] and the length of ordinary Cr–S bonds (2.399 and 2.466 Å) in electron-saturated complex $\mathrm{Cp(CO)_3Cr}-\overrightarrow{\mathrm{S}-\mathrm{S}-\mathrm{Cr}}\mathrm{(CO)_2Cp}$ [11].

Experimental

All operations were carried out under purified argon. The solvents benzene, heptane and hexane were purified by distillation over Na in a stream of pure argon. IR spectra were measured with a Specord IR-75 in KBr pellets. Magnetic measurements were carried out by Faraday's method with an instrument of the Institute of

Table 6

Bond angles ω (°) in the molecule $(MeC_5H_4)_2Cr_2(\mu_3\text{-}S)_2(\mu_4\text{-}S)Co_2(CO)_4$ (IIa)

Angle	ω	Angle	ω
Cr(1)Co(1)Cr(2)	58.02(6)	S(1)Co(2)S(3)	100.5(1)
Cr(1)Co(1)S(1)	57.18(9)	S(1)Co(2)C(21)	119.1(4)
Cr(1)Co(1)S(2)	55.13(9)	S(1)Co(2)C(22)	114.4(4)
Cr(1)Co(1)C(11)	158.5(4)	S(3)Co(2)C(21)	110.1(4)
Cr(1)Co(1)C(12)	103.4(4)	S(3)Co(2)C(22)	116.9(4)
Cr(2)Co(1)S(1)	56.77(9)	C(21)Co(2)C(22)	96.8(6)
Cr(2)Co(1)S(2)	55.63(9)	Co(1)Cr(1)Co(2)	100.09(7)
Cr(2)Co(1)C(11)	101.4(4)	Co(1)Cr(1)Cr(2)	60.64(6)
Cr(2)Co(1)C(12)	161.4(4)	Co(1)Cr(1)S(1)	51.86(8)
S(1)Co(1)S(2)	100.9(1)	Co(1)Cr(1)S(2)	52.86(8)
S(1)Co(1)C(11)	119.4(4)	Co(1)Cr(1)S(3)	116.5(1)
S(1)Co(1)C(12)	113.9(4)	Co(2)Cr(1)Cr(2)	60.62(6)
S(2)Co(1)C(11)	109.6(4)	Co(2)Cr(1)S(1)	51.98(8)
S(2)Co(1)C(12)	116.8(4)	Co(2)Cr(1)S(2)	116.4(1)
C(11)Co(1)C(12)	97.1(5)	Co(2)Cr(1)S(3)	52.38(9)
Cr(1)Co(2)Cr(2)	57.95(1)	Cr(2)Cr(1)S(1)	56.37(9)
Cr(1)Co(2)S(1)	57.05(9)	Cr(2)Cr(1)S(2)	55.97(9)
Cr(1)Co(2)S(3)	54.70(9)	Cr(2)Cr(1)S(3)	56.03(9)
Cr(1)Co(2)C(21)	158.4(4)	S(1)Cr(1)S(2)	94.1(1)
Cr(1)Co(2)C(22)	104.0(4)	S(1)Cr(1)S(3)	94.3(1)
Cr(2)Co(2)S(1)	56.68(9)	S(2)Cr(1)S(3)	87.2(1)
Cr(2)Co(2)S(3)	55.50(9)	Co(1)Cr(2)Co(2)	101.10(7)
Cr(2)Co(2)C(21)	101.3(4)	Co(1)Cr(2)Cr(1)	61.34(6)
Cr(2)Co(2)C(22)	161.9(4)	Co(1)Cr(2)S(1)	52.33(8)
Co(1)Cr(2)S(2)	52.40(9)	Co(1)S(1)Cr(2)	70.9(1)
Co(1)Cr(2)S(3)	116.6(1)	Co(2)S(1)Cr(1)	71.0(1)
Co(2)Cr(2)Cr(1)	61.43(6)	Co(2)S(1)Cr(2)	70.8(1)
Co(2)Cr(2)S(1)	52.49(8)	Cr(1)S(1)Cr(2)	66.28(9)
Co(2)Cr(2)S(2)	116.9(1)	Co(1)S(2)Cr(1)	72.7(1)
Co(2)Cr(2)S(3)	52.56(9)	Co(1)S(2)Cr(2)	72.0(1)
Cr(1)Cr(2)S(1)	57.35(9)	Cr(1)S(2)Cr(2)	68.3(1)
Cr(1)Cr(2)S(2)	55.71(9)	Co(2)S(3)Cr(1)	72.9(1)
Cr(1)Cr(2)S(3)	55.42(9)	Co(2)S(3)Cr(2)	71.9(4)
S(1)Cr(2)S(2)	94.6(1)	Cr(1)S(3)Cr(2)	68.6(1)
S(1)Cr(2)S(3)	94.6(1)	Co(1)C(11)O(11)	176(1)
S(2)Cr(2)S(3)	86.6(1)	Co(1)C(12)O(12)	178(1)
Co(1)S(1)Co(2)	134.0(1)	Co(2)C(21)O(21)	178(1)
Co(1)S(1)Cr(1)	71.0(1)	Co(2)C(22)O(22)	177(1)

General and Inorganic Chemistry of Academy of Sciences of the U.S.S.R. Experimental data for the X-ray study were obtained with an automatic Hilger and Watts diffractometer (λMo-K_α λMo 0.71069 Å, θ–2θ scan, $2 \leqslant 2\theta \leqslant 60°$, T 293 K). Crystals of II are monoclinic, space group $C2/c$, a 15.246(1), b 11.846(9), c 9.9434(6) Å, β 100.965(6)°, V 1763.0 Å^3, $Z = 4$. Crystals of IIa are triclinic, space group $P\bar{1}$, a 9.9771(9), b 10.1120(10), c 11.0770(10) Å, α 116.982(8), β 99.560(8), γ 82.054(8)°, $V = 979.5$ Å^3, $Z = 2$. The intensities of 2321 or 2997 reflections were measured for II or IIa, respectively, of which 1871 and 2935 with $I \geqslant 2\sigma$ were used considered observed. The structures were solved by direct methods and refined by full-matrix least squares to an anisotropic approximation for all non-hydrogen atoms ($R = 0.046$ and $R_w = 0.057$ for II; $R = 0.049$ and $R_w = 0.051$ for IIa). All calculations were carried out with an Eclipse S/200 computer using INEXTL programs [12].

$(C_5H_5)_2Cr_2(\mu_3\text{-}S)_2(\mu_4\text{-}S)Co_2(CO)_4$ (II)

A solution of 0.5 g (1.12 mmol) of $Cp_2Cr_2(SCMe_3)_2S$ [13] and 0.39 g (1.14 mmol) of $Co_2(CO)_8$ in 30 ml of benzene was heated at 45–50 °C for 5 h, the colour of the solution changed from violet into brown. The solution obtained was filtered, and 10 ml of heptane added, then concentrated to 5–10 ml at 30 °C/10 Torr, and allowed to stand at −5 °C. The precipitated dark-brown fine-crystalline powder was separated from solution, washed with hexane and dried in vacuum. Yield 0.16 g (26%). Monocrystals for X-ray study were obtained by diffusion of heptane into a solution of II in CH_2Cl_2. IR spectrum (ν, cm^{-1}): 515m, 680w, 818m, 1040w, 1420m, 1940vs, 1980vs, 3080w.

$(MeC_5H_4)_2Cr_2(\mu_3\text{-}S)_2(\mu_4\text{-}S)Co_2(CO)_4$ (IIa)

To the violet solution of 1 g (2.11 mmol) of $(MeC_5H_4)_2Cr_2(\mu\text{-}SCMe_3)_2(\mu\text{-}S)$ [14] in 10 ml of heptane was added a solution of 0.72 g (2.21 mmol) of $Co_2(CO)_8$ in 20 ml of heptane at 20 °C. The brown solution obtained was concentrated at 30 °C/0.1 Torr to 1/5 of its volume and allowed to stand overnight at 0 °C. The precipitated brown prisms were separated from solution, washed with cold pentane and dried in vacuum. Yield 0.6 g (49%). IR spectrum (ν, cm^{-1}): 460m, 480m, 522m, 600w, 815m, 835m, 1020m, 1050w, 1360m, 1418m, 1422m, 1480w, 1945vs, 1975vs, 3080w.

References

1 A.A. Pasynskii, I.L. Eremenko, O.G. Ellert, V.M. Novotortsev, Yu.V. Rakitin, V.T. Kalinnikov, V.E. Shklover and Yu.T. Struchkov, J. Organomet. Chem., 234 (1982) 315.
2 A.A. Pasynskii, I.L. Eremenko, B. Orazsakhatov, Yu.V. Rakitin, V.M. Novotortsev, O.G. Ellert, V.T. Kalinnikov, G.G. Alexandrov and Yu.T. Struchkov, J. Organomet. Chem., 210 (1981) 385.
3 A.A. Pasynskii, I.L. Eremenko, B. Orazskhatov, G.Sh. Gasanov, V.M. Novotortsev, O.G. Ellert, Z.M. Seifulina, V.E. Shklover and Yu.T. Struchkov, J. Organomet. Chem., 270 (1984) 53.
4 A.A. Pasynskii, I.L. Eremenko, B. Orazsakhatov, Yu.V. Rakitin, V.M. Novotortsev, O.G. Ellert, V.T. Kalinnikov, G.G. Alexandrov and Yu.T. Struchkov, J. Organomet. Chem., 214 (1981) 351.
5 I.L. Eremenko, A.A. Pasynskii, V.T. Kalinnikov, Yu.T. Struchkov and G.G. Alexandrov, Inorg. Chim. Acta, 52 (1981) 107.
6 M.D. Curtis, P.D. Williams, Inorg. Chem., 22 (1983) 2661.
7 R. Hoffman, J. Chem. Phys., 39 (1963) 1397.
8 J.H. Ammeter, H.-B. Bürge, J.C. Thibeault and R. Hoffmann, J. Amer. Chem. Soc., 100 (1978) 3686.
9 I.B. Bersuker, Electron structure and properties of coordination compounds, Khimiya, Leningrad, 1976.
10 V.G. Andrianov, B.P. Biryukov and Yu.T. Struchkov, Zh. Strukt. Khim., 10 (1969) 1129.
11 L.Y. Goh, T.W. Hambley and G.B. Robertson, J. Chem. Soc., Chem. Commun., 23 (1983) 1458.
12 R.G. Gerr, A.I. Yanovsky and Yu.T. Struchkov, Kristallographiya, 28 (1983) 1029.
13 A.A. Pasynskii, I.L. Eremenko, Yu.V. Rakitin, V.M. Novotortsev, V.T. Kalinnikov, Yu.T. Struchkov and G.G. Alexandrov, J. Organomet. Chem., 165 (1979) 57.
14 A.A. Pasynskii, I.L. Eremenko, Yu.V. Rakitin, V.M. Novotortsev, O.G. Ellert, V.T. Kalinnikov, V.E. Shklover, Yu.T. Struchkov, S.V. Lindeman, T.Kh. Kurbanov and G.Sh. Gasanov, J. Organomet. Chem., 248 (1983) 309.